Research paper ■

Molecular Imaging by Proton Magnetic Resonance Imaging (MRI) and MR Spectroscopic Imaging (MRSI) in Neurodegeneration

Rakesh Sharma

Abstract. Proton magnetic resonance imaging (MRI) and proton magnetic resonance spectroscopic imaging (MRSI) as integrated method was used to investigate NAA, creatine and choline changes in brain metabolites in Alzheimer's disease and epilepsy. Multislice H-1 MRSI technique of human brain, without volume preselection was used. Furthermore, MRI segmentation and completely automated spectral curve fitting facilitated quantitative data analysis in Alzheimer's disease and molecular imaging basis of prediction for epilepsy at different locations in the brain. MRI and MRSI integrated method was evaluated to characterize the anatomical and metabolite changes in disease.

■ **Infor Med Slov**: 2005; 10(1): 35-55

Author's institution: Magnetic Resonance Spectroscopy center, DVA Medical Center, San Francisco.

Contact person: Rakesh Sharma, Magnetic Resonance Spectroscopy center, DVA Medical Center, 4150, Clement Street, San Francisco, CA 94121. email: rs2010@Columbia.edu.

Introduction

MRI segmentation and co-analysis with H-1 MRSI appears to predict spectral peak variation due to brain tissue composition enclosed in a MRSI voxel which can mimic changes of the metabolite peak intensities. So, quantitative analysis of H-1 MRSI data should be able to distinguish the pixel intensity changes due to changes of the metabolite concentration from the intensity changes due to artifacts of partial volume effects. However, decreased NAA along with elevated Cho may be useful in differentiating axonal losses due to myelin breakdown from other segmented MR images.[1] The analysis includes point spread function and chemical shift displacement effects. Earlier, contributions to the observed NAA resonance from gray matter (GM) and white matter (WM) after nulling cerebrospinal fluid (CSF) or regions outside the brain was reported for application to brain tissue analysis.[2] The tissue content $\rho=(GM+WM)$ and an index for the gray matter $f=GM/(GM+WM)$. The NAA intensity correction for tissue volume was reported as $NAA^{corrected} = NAA/\rho$. The index f is used in statistical data analysis to account for variations of GM/WM voxel composition. Proton MRSI measures the regional distribution of important cerebral metabolites at much coarser spatial resolution than MRI due to sensitivity reasons. Mainly three amino acid metabolites are MRS visible from N-acetyl aspartate (NAA), choline (Cho) and creatine (Cr). NAA is found in neurons exclusively hence remains undetectable in other cell types. The Cho resonances in H-1 MR brain spectra originate predominantly from choline itself and from glycerophoshocholine and phosphocholine. These compounds are constituents of membrane phospholipids metabolism. Cho is known to increase markedly after myelin erosion.[3] Hence, choline is suspected to axonal losses not associative with myelin breakdown. Creatine resonance represents the sum of creatine and phosphocreatine that are both present in neural and glial cells.

H-1 MRSI using single volume pre-selection localization by PRESS method is significant in predicting epilepsy sensitive regions such as mesial temporal lobe, right and left hippocampus. In this paper, application of proton MRSI and MRI techniques is described to study neurodegenerative diseases such as Alzheimer's disease (AD), possibility of better classification of epilepsy using MR spectroscopic imaging such as mesial lobe epilepsy (MLE) and temporal lobe epilepsy (TLE). In AD, MRI showed a general loss of cortical tissue and volume reduction of hippocampus, a region involved in predictable memory functioning. Similarly, MRI studies showed tissue losses in the region of seizure focus i.e. in the hippocampus or in the neocortex of TLE patients. Although these anatomical changes are useful in diagnosis, they are not conclusive.

Principles of MRSI and metabolite imaging: Spatially selective RF excitation pulses in 3 orthogonal directions are applied on brain to get transient NMR time-domain signal which is further transformed into frequency domain signal intensity by Fourier transform of the acquired data. These NMR resonance frequencies of different contents, f (in Hertz), is defined by

$$f = \gamma(B_o - B_{electron}) = -\gamma B_o(1-\sigma), \qquad \text{Eq.1}$$

where the term σ is electron shielding effect or chemical shift of molecules oriented in Bo field. However, in vivo imaging only scalar component of motional averaging effect is measured. Based on the chemical $-CH_3$, $-CH_2$ or $-CH=$ groups, the spectral chemical shift peaks are generated and chemical shift frequencies generate different metabolite images such as NAA, Cr and Cho images. These images also depend on B_o field strength, spin-echo time (TE), field strength resonant frequency due to sum of chemical shift and spin-spin interaction or J-coupling (hertz). However, long TE and transverse relaxation T2 reduce complex and overlapping spectrum peaks of different insignificant metabolites.

Water resonance is used as internal standard based on using series of Rf pulses and gradient

pulses to achieve water magnetization spread over all phase angles in transverse plane. If water is suppressed, 1H spectrum and images are dominated by three singlet resonances from the protons (–CH_3 groups) in NAA at 2.0 ppm, Cr at 3.0 ppm, PCr at 3.03 ppm and Cho at 3.2 ppm having long T2 values and visible at longer TE. These metabolites and other metabolites such as γ-aminobutyric acid, glutamine, myo-inositol, taurine, amino acids have been reported for neurodegeneration and demyelination.[4] Short TE 1-H spectra for proteins and short relaxing large weight molecules such as lipids have been visualized in multiple sclerosis, necrosis.[5]

Data acquisition **in MRSI:** 3D data set is acquired by slice excitation for metabolite resonances which are integrated over brain regions for all voxels to give co-registered image. Image dependence on signal amplitude, frequency shift, inhomogeneity, phase may be described as

$$S(k_x,k_y,t)=\int\int\Sigma\rho(x,y,r).\ e^{-i(\omega(r)+\gamma\Delta Bo(x,y))t + k_{xy}+Ø(r) + Ø(x,y)) - t/T2(r)}.ðx,ðy,ðr \quad \text{Eq.2}$$

where index r is resonance(s), ρ(x, y, r) is signal amplitude distribution for each resonance, $\Delta B_o(x,y)$ is a spatially dependent frequency shift due to magnetic shift inhomogeneity, γ gyromagnetic ratio, Ø(r) is phase of each resonance, Ø(x,y) is zero-order phase term, $T_2(r)$ is the transverse relaxation rate of each resonance which is spatially variant, k_x, k_y are spatial encoding terms. Commonly used gradient phase encoding in all spatial dimensions, predict k_x as 3D variant depends on encoding gradient G_x applied in time t_{enc} .

$$K_x = \gamma \int^{enc}{}_o G_x(t).t.\ ðt \quad \text{Eq.3}$$

Images of NAA, Cr and Cho metabolite distribution can be generated by integrating over corresponding spectral regions for all points in spatial dimensions. Time deconvolution corrects time-varying values of $\Delta B_o(x,y)$ due to gradient eddy currents.

Co-analysis of MRI and MRSI: It is difficult to get 100% pure MR signal from one tissue due to mixed tissue distribution, partial volume contribution. It effects metabolite quantitation. Coanalysis of MRSI data from co-registered high resolution tissue segmented MRI data minimizes mixed signal effects such as CSF nulling and tissue fractional analysis by segmentation techniques.[5] However, Rf coil sensitivity distribution and volume selection profiles contribute to the signal from each voxel. By convolution of MRSI SRF with tissue distribution function and color coding 2D data of slice selection profile as a function of chemical shift offset of each metabolite may be described. For tissue, t, contributing to a voxel at position (x,y) for metabolite, m, in a 2D MRSI data set at slice position, z, the effective volume may be described as

$$V_{t,m}(x,y,z)=\Sigma I_t(x',y',z')SRF(x-x',y-y').P_m(z-z')C_m(x',y',z') \quad \text{Eq.4}$$

where I_t is the MRI-resolution distribution function for tissue type t; Pm is the slice-selective profile, which will vary as a function of the chemical shift of the selected metabolite resonance; and Cm represents additional factors of intensity distribution, Rf coil sensitivity and volume selection methods. Indices x' and y' cover the SRF within the image plane for the voxel (x,y) and z' must span all MRI slices that cover the MRSI slice selection profile. However, we used this analysis for separate signal contributions from white matter and gray matter. The signal of each metabolite can be described as

$$S_m(x,y,z)=\Sigma V_{t,m}(x,y,z)\rho_{tm} \quad \text{Eq.5}$$

where ρ_{tm} is signal for metabolite m and tissue type t which has been assumed regionally invariant over the selected voxels. The distribution of gray matter and white matter and CSF may be analyzed by multiparametric linear regression and further extrapolation to calculate 100% of each tissue and metabolite signal ρ_{tm}. Finally, co-registration of this data to nonlinear spatial transform into coordinate system. In present report, coanalysis of metabolite levels with volume measurements of

brain regions obtained from MRI included hippocampal volume for lateralization of epilepsy and ventricular or hippocampal volume reduction in Alzheimer's disease are reported. However, the analysis suffers from inaccuracy due to spatial variations of tissue distribution even in normal brain.

Methods and Materials

AD Patients and control subjects: Twelve patients (mean age ± s.d. 74.3 ± 8.0 years), ranged from 55 to 82 years old (8 females, 4 males) with the diagnosis of AD (9 probable, 3 possible AD) and 17 cognitively normal subjects of similar age and sex distribution were studied. The subjects were recruited from the different Alzheimer local centers, were examined by a neurologist, and had the standard battery of blood and neuropsychological test at the centers. The 17 control subjects had an evaluation similar to that of the AD patients and were judged to be normal cognition and function. None of the patients or controls had evidence of stroke, cortical or subcortical infarctions, or other major abnormalities on MRI scan which a neurologist reads. The combined MRI/MRSI protocol was completed by all control subjects and by 10 AD patients, while two patients did not complete MRI scan.

Mild Cognitive Impairment (MCI): Seven subjects (mean age ± s.d.; 72.8 ± 10 years range 56 to 85, 4 females, 3 males) who were not demented according to the Diagnostic and Statistical Manual of Mental Disorders (DSM-IV) criteria, presenting mild impairments of memory and/or cognitive functions, and having a Clinical Demetia Rating Score of 0.5 were selected for this study. These data were compared to 7 age matched cognitively normal subjects with a similar sex distribution (5 females, 2 males). The MCI subjects were recruited from the Alzheimer's centers, were examined by a neurologist, and had the standard battery of blood and neuropsychological tests at centers. The control 7 subjects had an evaluation similar to that of the MCI subjects and were judged to be normal cognition and function. No subject had evidence of stroke, cortical or subcortical infarctions, or other major abnormalities on MRI scans which were read by a neuropsychologist.

Diagnostic MRI examination: All studies were performed on a 1.5 Tesla Magnetom VISION system (Siemens Inc. Iselin, NJ) equipped with standard quadruple head coil. To minimize motion of the patient head, a vacuum-molded head holder (VacPac, Olympic Medical, Seattle WA) was employed to restrict head movements. The MRI protocol consisted of sagittal T1 weighted localizer scans, oblique axial double spin echo (DSE) scans angulated parallel to the optic nerve as seen in the sagittal plane, and a volumetric (3D) magnetization prepared for rapid gradient echo (MP-RAGE) acquisition angulated perpendicular to the DSE image planes. These examinations yielded T1-weighted coronal images estimated to be orthogonal to the long axis of the hippocampus. The measurement parameters of DSE were: TR/TE1/TE2 = 300/20/80 ms, 1.0 x 1.4 mm^2 resolution, and 48 to 51 contiguous 3 mm thick slices, covering the entire brain from the inferior cerebellum to the vertex. The measurement parameters of 3D MP-RAGE were TR/TI/TE=10/250/4 ms, flip angle 15,1.0 x 1.0 mm^2 resolution, and 1.4 mm thick partitions.

MRSI acquisition methods

All magnetic resonance studies were performed on a whole body 1.5 T Magnetom and magnetic resonance spectroscopic system. Multisection Spectroscopic Imaging (MSSI) and Point-resolved Spectroscopy (PRESS) were used. CHESS pulses were used in MSSI sequence. For MRI, magnetic resonance slices were angulated along the canthomeatal AC-PC line. 20 contiguous sections of 5 mm slice thickness and 0.5 mm section gap, TR=3000 ms, TE=30 and 80 ms were obtained to cover the entire brain from cerebellum to vertex. The magnetic resonance images were qualitatively evaluated without knowledge of subject's

diagnosis. Ventricular dilatation and sulcus widening were rated as mild, moderate and severe. Similarly, white matter signal hyperintensity (WMSH) were observed on the tip of lateral ventricles or periventricular rims or subependymal or subcortical regions. After MRI, acquisition of MRSI 17 mm-thick volume of interest (VOI) corresponding in location and thickness to the three MRI slices superior to lateral ventricles were selected for H-1 MRSI. The anterior-posterior and left-right dimensions of the H-1 MRSI volume of interest were adjusted according to the brain size. The position of a typical VOI 180 mm^2, phase-encoding 16 x 16, in-plane resolution 11 mm, spectroscopic volume 2.2 ml were obtained in 34 minutes.

Magnetic resonance imaging segmentation and hippocampal volume measurements

Magnetic segmentation and voluming: Tissue segmentation on the whole brain and voluming of the hippocampus was performed using software Spectroscopic Imaging Display (SID), developed in home laboratory. The semi-automated segmentation software was used for both 3D T1-weighted MP-RAGE and T2-weighted spin echo images. The first pass segmentation procedure automatically removes the skull and meninges from the images as shown in Figure 1. It co-registers the 3D T1 weighted images with each of the two interleaved spin-echo images.[6] It performs 3D inhomogeneity correction using a digital filter and performs the segmentation on the whole brain using K-means cluster analysis via the SAFASTCLUS procedure.[7] For this cluster analysis, seeds for each tissue category, i.e. gray matter (GM), white matter (WM), and cerebrospinal fluid (CSF), were first defined based on the regions around the peaks in the T1 pixel intensity histogram. These regions represented the conservative estimates of the approximate tissue category.[8] The initial process was followed by mutual editing of the data to separate cortical pixels from subcortical GM, ventricular CSF from sulcal CSF. This process reclassified those pixels incorrectly classified as GM into a category of white matter signal hyperintensity. The number of pixels for each tissue category was expressed as a percentage of total intracranial volume (TIV = total number of pixels).

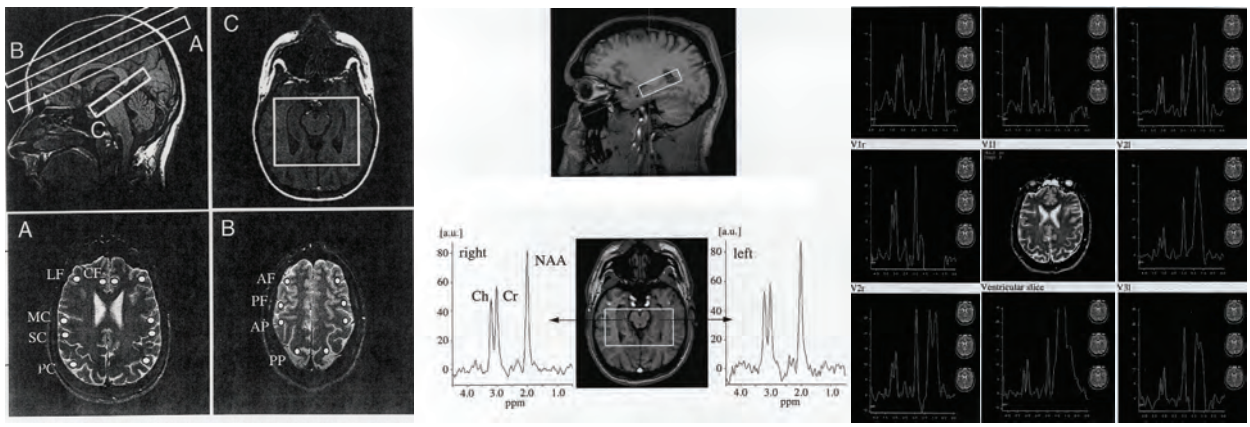

Figure 1 A localizer sagittal image (left on top), location of VOI (second on left) and different brain regions (left on bottom), corresponding spectrum at left and right locations (panels in center) and spectral peaks from 8 locations (panels on right) are shown to analysis tissue composition and metabolite concentrations in AD.

Quantitative estimates of the volumes of right and left hippocampus were obtained by using coronal T1-weighted MP-RAGE images. These images resliced the whole hippocampus perpendicular to the long axis of the hippocampus. Boundaries of the hippocampus were drawn.[6] The area of hippocampus in all regions of interest was automatically calculated and multiplying that

value by the slice thickness derived the total volume. The operator who was blinded to the patient's diagnosis performed all volume measurements. To adjust for inter-individual variations in head size, each subject's hippocampal volume (HV) was normalized to his or her intracranial volume index (TIV/TVI), which was the ratio of mean Total Intracranial Volume (TIV) in the control group and Total Intracranial Volume (TIV) in patient group, computed from the segmented images.[9] This procedure maintained the dimension of the normalized hippocampal volumes in contrast to the normalization calculated by 1/TIV. It was justified as long as the mean TIV values of the study groups are not significantly different. In this population, patients and control subjects had a comparable TIV values (difference $< 1\%$, $p < 0.96$ by ANOVA), suggestive of modest correlation between reduced TIV sizes and deficient cognitive functions.

MRSI postprocessing: After acquisition, the H-1 MRSI data were zero-filled to a rectangular matrix of 32 x 32 x 1024 points, Fourier transformed, and phase and baseline corrected using software developed in home laboratory. Four Hz Gaussian line broadening was used in the spectral direction, and mild Gaussian apodization was applied along the spatial direction to reduce Gibbs ringing effects, resulting in an effective volume of the MRSI voxels of approximately 1.6 ml. Voxels were selected from head, body, tail of the right and left hippocampus and the resonances from NAA, Cr and Cho were curve-fitted using NMR1 software (New Research Methods Inc. Syracuse, NY). In order to estimate the absolute concentrations in mmol/L, integral values of the metabolite resonances were referenced to the values obtained from a head-sized phantom, including corrections for coil loading, receiver gain, and metabolite T1 and T2 values from the H-1 MRS study in healthy elderly for gray and white matter.[10]

To obtain atrophy corrected metabolite intensities and to verify that metabolic changes were not an artifact of partial voluming, all MRSI data in this study were analyzed for variation in voxel compositions in terms of GM, WM, and CSF using SID software developed in house. This computation method analyzed the tissue segmented images. These tissue segmented images were co-registered with the MRSI data to estimate the composition of tissue in the MRSI voxel.[11,12] The computation was performed with the consideration of the MRSI point spread function, chemical shift displacement effects, and signal sensitivity across the PRESS volume, which was determined experimentally on a head sized phantom.[12] Assuming that no metabolites are observed in CSF, the composition of each MRSI voxel was characterized by the two parameters tissue content $\rho = (GM + WM)$ and gray matter index $f = GM/(GM + WM)$. Then, atrophy corrected metabolite intensities, i.e. of NAA, were computed according to $NAA = NAA^* \; 1/\rho$, with NAA* being the uncorrected intensity and "f" was used as covariate for the statistical analysis to determine the extent to which tissue composition contributed to metabolic differences.[13]

Typically, MRSI spectra from the hippocampal-body exhibited a better spectral resolution than spectra from hippocampal-head which often suffered from poor B_0 field homogeneities in this region.[14] Furthermore, hippocampal-head contained more GM tissue instead of the voxels from the tail, reflecting the brain anatomy in this region. So, MR spectra from the hippocampus-body were used exclusively for the further analysis.[15]

Statistical Analysis: Repeated measures of analyses of variance (ANOVA, SA Institute Inc. Cary, NC) were used to test group differences of hippocampus volumes and grossly atrophy measures. Analysis of covariance (ANCOVA, BMDP Statistical Solutions Inc. Ireland) was used with tissue composition f as covariate, to test by group and side by side differences of metabolite concentrations in right and left hippocampus.[16] In order to determine the extent that hippocampal NAA and volume were independent of each other, NAA was used as the independent variable. Hippocampus volume was used as covariate with NAA to determine their group membership by

ANCOVA.[17] Results were expressed as mean ± s.d. with standard error unless otherwise indicated. The level of significance for the differences was $p < 0.05$.

Comparison between neocortical epilepsy (NE) and mesial lobe epilepsy (mTLE) patients

Epilepsy Patients and control subjects: Ten subjects with available data on medically refractory NE (based on previous seizure semilogy and ectal EEG recording) were studied. The age range was 25-51 years (mean age 34.4 ± 7.4 years). All patients were first evaluated at the Epilepsy centers. At epilepsy center, the seizure focus was localized by scalp (including sphenoid electrodes) as necessary subdural electrode recordings.[18] Only patients were included whose ictal recordings were demonstrated either by localized voltage attenuation or rhythmic sharp activity that preceded or coincided with the onset of the clinical seizure. Among these patients, four had their seizures arose from the frontal lobe neocortex, two from the occipital lobe neocortex, one from the parietal lobe neocortex and three had their seizures arise from the lateral temporal lobe neocortex. The severity and frequency of seizures were similar in the NE patients and mTLE patients who were used for study. The NC and mTLE patients consisted of 23 unilateral medically refractory mTLE patients. The age range was 14-49 years (mean age 35 ± 9.7 years). Both NE and mTLE patients were compared to 16 healthy, age and sex matched controls (mean age range 23-56 years; mean age 33.3 ± 7.9 years).

Diagnostic MRI and MRSI analysis: All the NE patients had normal MRI. Both hippocampi were normal in appearance, shape and volume. In 8 out of 10 patients absolute concentrations were concluded using the unsuppressed water resonance as a reference. The concentration of metabolites included metabolite-corrections and water signals for T1 and T2 relaxation, and corrections for the number of protons belonging to the metabolite resonances. EEG findings were used as a standard for localization and lateralization of the seizure focus. Lateralization by MRSI was performed in several ways: The NAA, choline and creatine concentrations (NAA, Cho and Cr) and metabolite ratios (NAA/Cr, NAA/Cho, and NAA/(Cho+Cr) were compared between left and right hippocampi of the patients. Furthermore, the patient's values were compared to control's values. Asymmetry indicies were calculated by $(M_{contra}–M_{ipsi})/(M_{contra}+M_{ipsi})100$ for patients and $(M_{left}–M_{right})/M_{left}+M_{right})100$ for controls, with the metabolite concentration or metabolite ratio designed by M.

Statistical Analysis: Statistical analysis of the MRSI data comparing metabolite concentrations and ratios between NE and mTLE patients and controls were done using a one tailed unpaired t-test. A probability value of $p < 0.05$ was considered significant for each analysis. In order to detect also smaller metabolite changes we did not correct for multiple comparisons. All data are presented as mean ± s.d.

Post-operative mTLE patients' evaluation

Patients and control subjects: 10 patients with unilateral medically refractory mTLE based on seizure semiology and ictal EEG recording, were studied before and after surgery. A temporal lobe resection, including the anterior part of the hippocampus was performed on the ipsilateral side (defined by EEG telemetry, MRI and other clinical measures) in all patients. The age range was 24-49 years (mean age 34.6 ± 9 years). Eight of the patients were seizure free after temporal lobectomy (class I according to Engel's classification;[19] 2 patients had continued complex partial seizures following surgery (1 patient class II and I patient class III). Memory was evaluated using the Rey Auditory Early Learning Test (RAVLT), a widely used measure of verbal learning and memory. The patients were compared to healthy age and sex matched controls (age range 23-56 years; mean age 33.3 ± 7.9 years).

MRI and MRSI examination: All MRSI studies were performed on a 1.5 Tesla Magnetom VISION

(Seimen Erlangen) as previously described. The follow-up measurements were performed using exactly the same measurement protocol. In postoperative studies, the patients were carefully repositioned like the same orientation prior to surgery. The anterior border of the contralateral hippocampus was used pre- and postoperative as a hallmark for positioning of the PRESS box.

MRSI post-processing: The MRSI data were processed as described before. An average of 6 voxels centered primarily on hippocampus gray matter was selected. Metabolite concentrations were found to vary along the long axes of the hippocampus. Therefore, same co-registered voxel positions were postprocessed for pre- and postoperative sessions if the spectrum quality was sufficient at these positions. In addition, the selected voxels within the PRESS box were selected as good as possible at equivalent positions in the hippocampus. This postprocessing procedure excluded the possibility of detecting differences due to changes in metabolite concentrations between the anterior and posterior part of the hippocampus.

Quantitative data were calculated using the unsuppressed water signal as a reference. The corrections required for the quantitation - including corrections for the number of protons and relaxation times have been previously described. Furthermore, to compare also the water signal before and after surgery it was corrected for coil loading by multiplying the signal with the transmitter reference value.

Statistical Analysis: Statistical analysis of the MRSI data were compared for the metabolite concentrations and ratios between patients for the pre-and postoperative sessions. Analysis was done for the patients and controls using ANOVA (SAS Institute Inc.Cary, NC). The p-values were calculated using two tailed paired t-tests and unpaired t-tests for comparisons between pre- and postoperative data and comparison between patients and controls, respectively. However, when comparing the three groups (patients pre- and postoperative and controls) statistical significance was assumed only for probability values of $p < 0.05$ using the Tukey's test to examine all pair-wise comparisons among means. All data are presented as mean ± s.d.

Combined multislice and PRESS **MRSI in mTLE patients:** MRSI studies were performed on 9 patients with unilateral mTLE based on ictal semiology and EEG recording, which was defined as ipsilateral side. Seven healthy volunteers were included as controls with sex and age matched data. The MRSI studies were done on a 1.5 Tesla Magnetom VISION (Seimen Erlangen) using a standard circularly polarized head coil.

Diagnostic MRI and MRSI: Multislice MRSI studies require excellent magnetic field homogeneity over a large region. Due to severe susceptibility B_0 shifts in the anterior temporal lobe and hippocampus, this region often requires a different shim than other brain areas. Therefore a separate PRESS volume-preselection experiment for the hippocampal region was performed using a separate shim. The slice was angulated parallel to the long axis of the hippocampus, and a circular k-space encoding of 24 points diameter was used (TR/TE=1800/140 ms, nominal voxel: 9 x 9x 15 mm^3). The multi-slice experiment included two 15 mm slices acquired using a global shimming with a circular k-space encoding of 36 points diameter (TR/TE=1800/140 ms, nominal voxel size: 8 x 8 x 15 mm^3). Both slices were angulated parallel to the optic nerve with the lower slice just including the corpus-callosum and the other slightly above the corpus callosum. Lipid removal was performed by a data post-processing procedure.

Regression against tissue content and histogram analysis: Automated spectral fitting and automated MRI tissue segmentation after co-registration with MRSI were routine methods. Another factor was metabolite differences in GM, WM and WM signal hyperintensities (WMSH). Therefore, a regression analysis was done for the volume corrected (NAA) as a function of the GM tissue fraction within each MRSI voxel. An extrapolation to 100% GM yielded an estimate of NAA in pure GM. Similarly, an extrapolation to

100% WM yielded NAA in pure WM. Other method was based on the hypothesis that different progressive neurodegeneration stages were reflected by NAA concentration in the voxels across that brain region. For it, histogram analysis of atrophy corrected (NAA) values were obtained from parietal lobes which contained more than 70% GM with assumption that GM was effected maximum in AD.

Table 1 Clinical characteristics of patients with Alzheimer's disease (AD) and control subjects.

	AD	Control
Number of subjects	12	17
Mean Age (yrs)*	72.5 ± 9.8	73.1 ± 5.1
Age Range (yrs)	52 - 80	60 - 82
Women/Men	8 / 4	14 / 3
Mini-Mental State*	16.9 ± 5.6	29.7 ± 1.2
Mini-Mental State Range	14 - 21	27 - 29
Mean duration of the symptoms (yrs)*	4.4 ± 1.4	---

Table 2 Atrophy corrected metabolite concentrations of NAA, Cho, and Cr and NAA/Cr and NAA/Cho ratios from right and left hippocampus in AD patients and control subjects. Tissue content ρ (in percent of the MRSI voxel volume) and gray matter index f of the MRSI voxels positioned at right and left hippocampus, characterizing MRSI partial volume effects.

	AD	Control	p-value
HP-Vol. (mm^3) Right	1982 ± 134	2884 ± 102	0.003
HP-Vol. (mm^3) Left	1868 ± 88	2943 ± 86	0.001
Ventricular CSF (%)	4.2 ± 0.3	2.8 ± 0.3	0.03
Sulcus CSF (%)	23.4 ± 2.1	18.2 ± 0.5	0.01
White Matter (%)	35.2 ± 0.9	38.1 ± 0.8	0.01
Cortical GM (%)	38.8 ± 1.1	42.2 ± 0.6	0.03
Subcortical GM (%)	1.2 ± 0.08	1.4 ±0.03	n.s.
TIV (cm^3)	1342 ± 35	1402 ± 52	n.s.

Results

Alzheimer's disease

Demographics: The demographic data is shown in Table 1. Patients and elderly controls were comparable in age ($p > 0.5$ by ANOVA) and had a similar gender distribution (67% vs 82% females in the patient and control group, respectively). The AD patients had a mean MMSE score of 18.4 ± 5.2 s.d. with the range from 12 to 28 and a mean duration of symptoms of 4.2 years ±1.8 years (mean ± s.d.). Elderly control subjects had MMSE scores of at least 28 or better.

MR Spectroscopic Imaging: Table 2 shows the results of atrophy corrected NAA, Cr and Cho and the ratios NAA/Cr and NAA/Cho from the left and right hippocampus in AD and control subjects. Data shows (% tissue composition in voxel) and f, revealing significant differences in the composition of MRSI voxels between the two groups. After correcting NAA atrophy in the right and left hippocampus in AD, the NAA was reduced by 15% and by 16.2% ($p < 0.003$) respectively, compared to the NAA in control subjects. Variations of tissue composition did not significantly contribute to the differences ($p > 0.98$). Furthermore, both NAA/Cr, NAA/Cho were significantly reduced ($p < 0.02$ and p value < 0.03 respectively) in AD compared with elderly controls. Reductions of NAA after NAA correction in AD could not be entirely attributed to the atrophy factor because of the multifactorial dependent nature of NAA. The concentrations of hippocampus Cr and Cho were not significantly different between AD and control subjects. In both groups, NAA, Cr and Cho concentrations were non-significantly higher in the left than in the right hippocampus ($p > 0.07$). MRSI voxels from AD contained an average 10% less tissue than in control subjects, reflecting the increased atrophy in AD. Accordingly, the difference of hippocampal NAA between the groups without atrophy correction (which reflects both NAA and volume changes) was about 40% larger than with correction of atrophy. This emphasizes the

importance of correcting MRS and MRSI data for partial volume effects.

Table 3 Normalized hippocampus volumes (HP-Volume) and volumes of cortical and subcortical gray matter (GM), white matter (WM), and fluid (CSF) as percent of total intracranial volume (TIV) in AD patients and control subjects.

	Concordant	Discordant	Non-lateralized
FDG-PET Asymmetry score (>3%)	12	0	1
HV (AI > 8%)	10	0	3
T2 (AI > 4%)	9	0	4
NAA/(Cho+Cr) (AI > 12%)	7	1	5
NAA (AI > 12%)	7	0	6

MRI Voluming and Segmentation: Table 3 represents the normalized hippocampal volumes in AD patients and elderly controls, as well as percent volumes of cortical and subcortical GM, WM and ventricular and sulcal CSF. As expected, AD patients had smaller hippocampi on both sides than control subjects, on the right 20.1% ($p<0.003$) and on the left 21.8% ($p < 0.001$) and the right hippocampus was slightly larger (~2%) than the left, but this difference was not statistically significant ($p<0.5$). In AD, ventricular and sulcal CSF volumes were enlarged by 34.1% ($p < 0.03$) and by 22.8% ($p > 0.01$), respectively, when compared to controls, and cortical GM and WM were reduced by 6.1% ($p < 0.03$) and by 7.3% ($p < 0.01$), respectively. In contrast, subcortical GM ($p > 0.6$) and total intracranial volume ($p > 0.06$) were not significantly different between AD and control subjects.

Combination of MRI and MRSI measures for AD: Figure 2 shows the distributions of hippocampal NAA< hippocampal volume and% ventricular size in AD and control subjects, separated by gender. It was observed that no single measurement alone provides a complete distinction of AD patient and control subjects. In order to explore this possibility, hippocampal NAA and volume were analyzed to get better information which may aid group classification as these two measures are independent of each other. After normalizing the group differences in hippocampal volumes by ANCOVA, significant differences of hippocampal NAA between the groups were still observed ($p<0.002$). Similarly, after controlling for group differences in hippocampal NAA, volume losses in AD remained significant ($p<0.001$). Taken together, these results revealed that hippocampal NAA and volume each provide independent information relevant to the discrimination of AD from control subjects. Figure 3 shows the distribution of atrophy corrected hippocampal NAA (right and left averaged) from each AD patients and control subjects as a function of their hippocampal volume (right and left averaged). To determine the classification power of hippocampal NAA and volume when combined, we performed a stepwise linear discriminant analysis with hippocampal NAA being the first variable entered. Alone, hippocampal NAA correctly classified 80% (8/10) of the AD and 75% (12/16) of the control subjects. When hippocampal volume was combined with NAA, the two measures increased the power for the classification of AD and control subjects to 90% (9/10) and 94% (15/16) respectively. Combining the two in addition,% ventricular CSF did not improve the classification of AD and decreased the classification of controls.

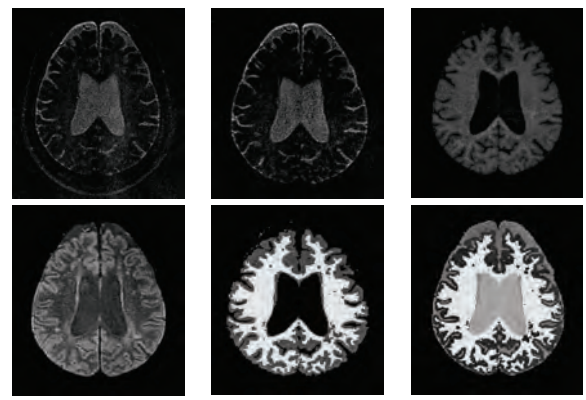

Figure 2 Brain images are shown before postprocessing (top panels) and after postprocessing (bottom panels) to demonstrate tissue analysis by segmentation for white matter, gray matter and CSF.

Table 4 Hippocampal lateralization and voluming as a test of discordance is analyzed in terms of metabolites to evaluate asymmetry scores volume (TIV) in AD patients and control subjects.

Metabolite	AD	Control	% Diff.	p-value
	NAA (mM)			
Right	7.55 ± 0.5	10.01±0.6	14	0.0001
Left	7.61 ± 0.4	9.82±0.9	12.6	
	Cho (mM)			
Right	2.02 ± 0.7	2.08 ± 0.2	1.46	n.s.
Left	2.04 ± 0.4	1.89 ± 0.5	3.8	
	Cr (mM)			
Right	7.02 ± 0.6	7.75 ± 0.5	4.9	n.s.
Left	7.96 ± 0.6	7.49 ± 0.8	3.0	
	NAA/Cr			
Right	1.08 ± 0.8	1.3 ± 1.2	9.2	n.s.
Left	0.96 ± 0.6	1.3 ± 1.1	15.0	
	NAA/Cho			
Right	3.74 ± 0.7	4.8 ± 3.0	12.4	n.s.
Left	3.73 ± 1.0	5.4 ± 1.8	18.2	
	Tissue content ρ (%)			
Right	84 ± 3	98 ± 2	7.6	0.005
Left	87 ± 3	96 ± 3	4.9	
	Gray matter index (f)			
Right	0.45 ± 0.03	0.55 ± 0.05	10	0.0001
Left	0.62 ± 0.02	0.62 ± 0.04	0	

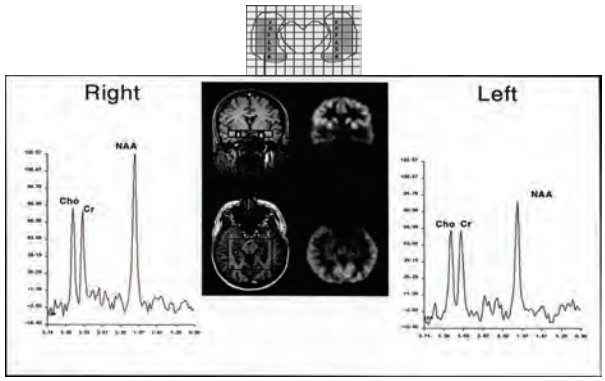

Figure 3 Coronal images showing distribution of atrophy corrected hippocampal NAA (right and left averaged), Cr and Cho from each AD patients and control subjects as a function of their hippocampal volume.

4.2 Epilepsy: Controls: Table 4 represents the mean values for each of the quantitative MR measures: hippocampal volume (HV), T2 relaxometry, NAA, NAA/(Cho+Cr). The mean HV for 19 control subjects (38 hippocampi) was 3452 mm^3. Although, the mean HV of the right lobe (3501 mm^3) was greater than the mean HV of the left lobe (3401 mm^3) hippocampi, the difference was not statistically significant ($p < 0.037$). No right-left differences were found for T2 and H-1 MRSI measures.

Table 5 Lateralization sensitivity in TLE patients based on HV defined hippocampal atrophy.

	Atrophy (n=12)	Without atrophy (n=7)
FDG-PET	11 (90%)	5 (70%)
NAA/(Cho+Cr)	10 (82%)	5 (70%)
NAA	10 (82%)	4 (60%)

Patients: Table 5 represents the ictal EEG and imaging results for the 5 patients. Results were represented as lateralized for each modality and these were based on generally conservative criteria for intermodality comparison of lateralization for each patient.

Table 6 Comparison of lateralization in Temporal Lobe Epilepsy (n=15) as test of discordance by using hippocampal volume, metabolites peaks.

	Concordant	Discordant	Non-lateralized
FDG-PET Asymmetry score (>3%)	20	0	3
HV (AI > 8%)	15	0	8
NAA/(Cho+Cr) (AI > 12%)	14	1	8
NAA (AI > 12%)	15	1	7

Metabolite measures for optimum lateralization in Epilepsy: In order to determine the best lateralization criteria, the concentrations of NAA, Cr and Cho, as well as metabolite ratios of NAA/(Cr+Cho), NAA/Cr, and NAA/Cho were evaluated. Statistical analysis showed no significant left to right differences in any metabolite concentrations or metabolite concentrations or metabolite ratio in the control group. In control and patient groups, no age- or

sex-related differences were found (values $p > 0.05$). In the TLE patients the NAA ratios and the NAA concentrations (NAA) observed as substantially decreased in the ipsilateral hippocampus. In addition, NAA measures were decreased in the contra-lateral hippocampus of TLE patients in comparison with controls. Hippocampal (NAA) was 11.6 ±1.3 mmol/L (mean ± 1 s.d.) in controls, 8.1 ± 1.5 mmol/L ($p < 0.002$) on the ipsilateral side, and 9.4 ± 1.3 mmol/L ($p > 0.0001$) on the contralateral side of TLE patients. Similarly, the mean NAA/(Cr+Cho) ratio was found to be 0.81 ± 0.06 in controls, 0.059 ± 0.1 ($p < .004$) in the hippocampus ipsilateral to the seizure focus, and 0.73 ± 0.13 ($p>0.05$) in the contralateral hippocampus in patients. The concentrations of Cr and Cho were not significantly changed in patients compared with the controls ($p > 0.08$). However, a trend for decreased [Cr] was found, with the mean ipsilateral [Cr] in TLE patients 10% less than in controls. The coil-loading metabolite signals yielded a slight increase in the ipsilateral Cho signal of 6.7% in patients, but no statistical significant difference was observed. Furthermore, although a decreased ipsilateral Cr/Cho was found for the TLE patients (ipsilateral mean Cr/Cho=0.90, control mean Cr/Cho=1.0). Lateralization analysis based on Cr/Cho was failed in 8 of 16 patients.

FDG-PET atrophy information, lateralization, and MRI findings is presented in Table 5. The table shows MRSI lateralization based on [NAA] and NAA/(Cr+Cho). Lateralization criteria included comparing left to right MRSI measures in TLE patients and TLE MRSI data compared with control data. The NAA/(Cr+Cho) ratio provided concordance with EEG lateralization in left to right comparison in all TLE patients. In 15 of 16 patients, both ipsilateral [NAA] and NAA/(Cr+Cho) mean ± s.d. values were less than mean ± 1 s.d. control values. The [NAA] did not lateralize correctly in 3 patients without atrophy, but showed greater bilateral abnormalities (i.e. abnormalities in both the ipsilateral and contralateral hippocampi) in comparison with control [NAA] values. Similar observations were common for the metabolite ratio measures. The NAA/Cho ratio failed to lateralize one patient correctly, and NAA/Cr failed to lateralize 3 patients. The NAA/(Cr+Cho) ratios and [NAA] values for ipsi-and contralateral abnormalities in TLE patients and left vs right comparison in controls are plotted as shown in images Figure 4 and 5.

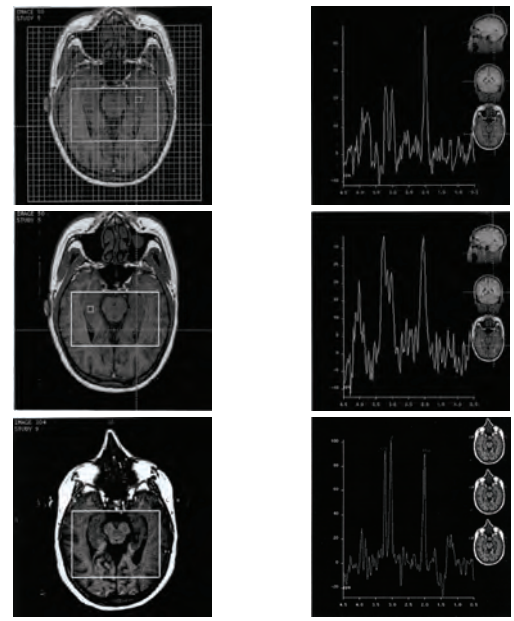

Figure 4 T1 axial images showing VOI and spectroscopic voxels and selective spectral peaks from right and left sides to compare metabolites in cortical and ventricular regions (peaks on right panels).

Relationship of decreased NAA to hippocampal atrophy: The second specific aim of this study was to determine if decreased hippocampal NAA in TLE is simply due to hippocampal atrophy. Figure 5 and 6 shows that 6 out of 7 subjects without hippocampal atrophy, as assessed by MRI, had decreased ipsilateral hippocampal [NAA]. These findings strongly suggest that decreased hippocampal NAA cannot be explained by atrophy alone. Because the water signal was used for absolute quantitation, the magnificent of the hippocampal water signal was analyzed. The TLE patient groups showed slightly increased mean ipsilateral hippocampal water signals (mean increase in patients with hippocampal atrophy:

7.9%; without hippocampal atrophy: 4.4%). This might be due to either increased cerebrospinal fluid water or increased T2 of water in the hippocampus. However, the mean ipsilateral water signal increase of 7.9% in TLE patients with atrophy accounted for only 6.5% of the 34.2% [NAA] decrease. Furthermore, no negative correlation between the water and the NAA signal was observed (correlation coefficient 0.26).

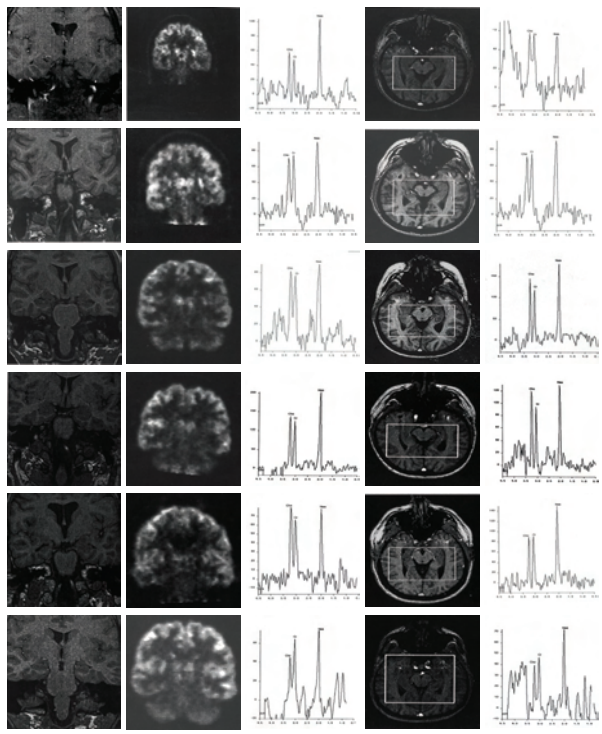

Figure 5 The prediction power of MRI (column A), NAA images (column B) and MRSI (for left vs right lateralization on columns C-D). Metabolite images are demonstrated with VOI box in column D on left vs right voxels selected.

Bilateral abnormalities: To determine the presence of bilateral hippocampal disease in TLE, MRSI data from the contralateral hippocampus were compared to controls. Mean contralateral [NAA] was significantly reduced below controls. Mean contralateral [NAA] was less than ± 1 s.d. below the control mean in 12 of 16 (75%) TLE patients. The NAA/(Cr+Cho), NAA/Cr and NAA/Cho ratios were below ±1 s.d. of the controls in 8 of 16 (50%) TLE patients.

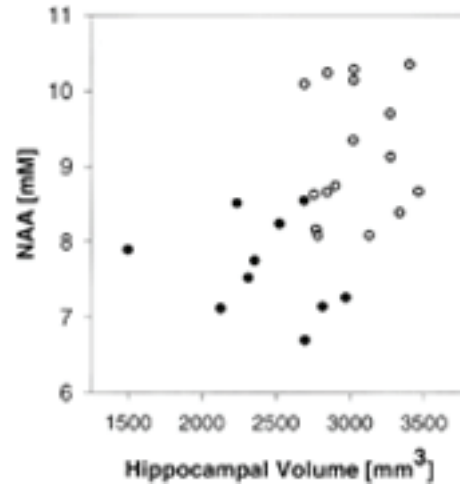

Figure 6 Data is shown for TLE epilepsy subjects without hippocampal atrophy, as assessed by MRI, had decreased ipsilateral hippocampal [NAA] on y axis.

Relationship of MRS data to surgical outcome in Epilepsy: One of the aims of these MRSI and MRI examination was to investigate the correlation between MRSI findings and seizure surgery outcome. 11/16 patients underwent surgery. Six patients with hippocampal atrophy had surgery and 5 became seizure free (five class I, one class III). Both [NAA] and [NAA/(Cr+Cho)] in these 6 subjects provided lateralization concordant with EEG. 5 patients without hippocampal atrophy had surgery. In two of them, [NAA] and [NAA/(Cr+Cho)] findings were concordant with EEG and they became seizure free (class I). In three remaining patients the NAA/Cr+Cho ratio lateralized concordant with EEG but NAA was equally low on both sides or was even lower on the contralateral side. These three patients continued to have seizures after surgery although the seizure frequency decreased. 4 of the 7 seizure-free patients also showed contralateral decreased [NAA] for the patients who were followed after seizure surgery as shown in Figure 5.

In summary, 7 unilateral TLE patients who underwent surgery, a contracordant decrease of

[NAA] and [NAA/(Cr+Cho)] in the ipsilateral hippocampus predicted the surgical success. 5 of these 7 patients had ipsilateral atrophy. In three subjects without ipsilateral atrophy, a bilateral equally decreased or contralateral lower [NAA] was associated with a poor surgical outcome.

Lateralization of lobes in Epilepsy: FDG-PET: 23 of 24 (96%) patients studied with PET had one or more regions with relative hypometabolism confined to a single TL. Because of the subjective nature of determining relative hypo-metabolism and the risk of false interpretation in the presence of asymmetric partial volume effects, several asymmetry thresholds were evaluated. PET with MRI co-registration was necessary to resolve lateralization in one patient. Requiring 3 or more regions of relative hypo-metabolism was a conservative but consistently reliable threshold for lateralization that resulted in 21 of 24 (88%) patients lateralized by FDG-PET with no discordance.

Diagnostic MRI: MRI revealed easily discernable relative hippocampal atrophy in 15 patients (66%) and unilateral increase in hippocampal T2 signal in nine patients (36%). None of these patients shows T2 hypersensitivity without hippocampal atrophy. In all cases MRI identified hippocampal atrophy was concordant with ictal EEG. All 25 patients had hippocampal examination. An atrophy index (AI) > 8% was caliberated as criteria to eliminate all discordance. With this threshold value of AI, 17/25 patients (68%) were lateralized. In 16 of 17 patients had concordant hippocampal atrophy more than ± 2 s.d. below the mean of control. To determine if the yield for accurate lateralization could be improved, a presumption was added that HV can be lateralized only if hippocampal volumes were more than ± 2 s.d. below the mean of controls. This presumption decreased the percent discordance for all atrophy index thresholds < 8%, but percent concordance remained lower. Thus, the optimum criterion for lateralization with hippocampal atrophy was an atrophy > 8% without any additional requirement for absolute abnormality.

T2 relaxometry: To eliminate all discordance an atrophy index > 4% was required. With this threshold, 9 of 13 patients (69%) were lateralized. If the presumption was added that T2 are lateralized only if it was more than ± 2 s.d. above the mean of controls, discordance was eliminated at all atrophy index values with the trade-off that sensitivity was decreased to 54%. Thus, the optimum criteria for T2 lateralization was atrophy index values, but it showed less sensitivity decreased to 54%. Thus the optimum criteria for T2 lateralization was atrophy index > 4% without any additional presumption for absolute abnormality.

H-1 MRSI: Both NAA/(Cr+Cho) and NAA included some discordance patients with relatively high asymmetry. An atrophy index > 16% was required to eliminate all discordance with NAA/(Cr+Cho). This resulted in 10 of 24 patients (42%) lateralized. Adding the requirement that NAA/(Cr+Cho) be lateralizing only if it was more than ± 2 s.d. below the mean of controls did not reduce the atrophy index that was required to eliminate discordance. With [NAA] lateralization, an atrophy index > 24% was required to eliminate all discordance, a threshold that resulted in a sensitivity of only 21%. AD with NAA/(Cr+Cho), adding the requirement that [NAA] be lateralizing only if it was more than ± 2 s.d. below the mean of controls did not reduce the atrophy index that was required to eliminate discordance. These data suggest that no optimum criteria for H-1 MRSI lateralization exist without including one or more cases discordant with ictal EEG. Because discordance is not necessarily an indication of false lateralization, we examined H-1 MRSI lateralization results in patients completely free of seizures (including auras or simple partial seizures) following surgery. In this subgroup of 15 patients, NAA/(Cr+Cho) discordance was present in 4 patients with atrophy index of 11%, 15% and 1%. None of the fifteen patients had discordant [NAA]. The mean atrophy index of normal controls was ± 2 s.d., approximately 20% for both H-1 MRSI measures. If the asymmetry threshold was based on this value, lateralization sensitivity was low about 27%

with NAA/(Cr+Cho) and 47% with [NAA] (n=15). Selective lateralization based upon the choosing side with the lowest value, regardless of degree of asymmetry, was unreasonable, even if only patients with abnormal values are counted.

Thus, H-1 MRSI measures the decision of optimized lateralization criteria remains arbitrary. In present study, an atrophy index > 12% seems a reasonable threshold for H-1 MRSI lateralization because NAA/(Cr+Cho) lateralization was simply unreliable with an atrophy index <12% (regardless of whether only patients with abnormal values are included). With this threshold applied to all 24 patients studied with NAA/(Cr+ Cho), the sensitivity was 58%, with discordant lateralization in one seizure free patient. The sensitivity for [NAA] was 63%, with discordant lateralization in one patient (no worthwhile improvement in seizures). Adding the presumption of including patients with H-1 MRSI values ± 2 s.d. below the means of controls only reduced sensitivity and did not increase discordance at lower asymmetry thresholds.

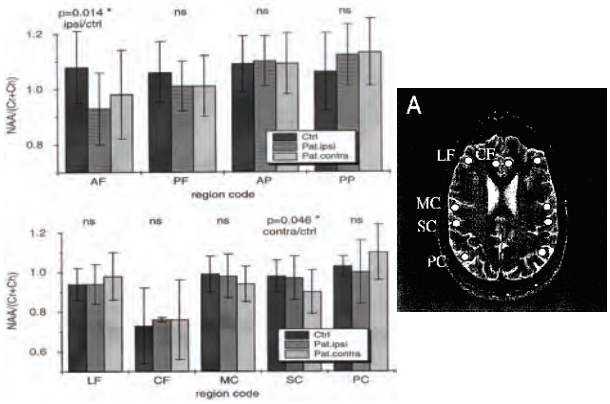

Figure 7 Metabolites in different regions of brain on ipsi and contralateral side (left) are compared in different locations of cortex (on right) of brain as the basis of asymmetry analysis and decision-making in mTLE epilepsy. Data is shown in Tables 7 and 8. Different parts of frontal lobe (LF), medial cortex (MC), subcortical (SC), parietal cortex (PC) is shown on brain image A (on right side).

Comparison of lateralization in mTLE:
Comparison of lateralization was performed in those patients who completed all examinations included in the evaluation study. Table 7 represents the lateralization from the 23 patients who completed FDG-PET, hippocampal atrophy and H-1 MRSI studies in all 25 patients. Using criteria described above, lateralization sensitivity was 87% with FDG-PET, 65% with hippocampal volumetry, 61% with NAA/(Cr+Cho) and 57% with [NAA]. With these criteria no discordance was found with FDG-PET or hippocampal voluming. Two patients were discordant with H-1 MRSI measures, one with NAA/(Cr+Cho) and the other with [NAA]. Table 7 represents the lateralization in patients grouped according to the presence or absence of hippocampal atrophy defined by hippocampal voluming. FDG-PET lateralized all but one (93%) of the 15 patients with hippocampal atrophy; each of the H-1 MRSI measures lateralized 10 (75%). NAA/(Cr+Cho) lateralization was discordant in one patient who has been seizure free since seizure surgery. Of the 8 patients without hippocampal atrophy, FDG-PET lateralized 6 (75%), NAA/(Cr+Cho) 4 (50%) and [NAA] 3 (38%) as shown in Figure 5 in 4-6 rows. The [NAA] lateralization was discordant in one patient who has had no worthwhile improvement in seizures since surgery. This patient was not lateralized by FDG-PET or NAA/(Cr+Cho). Utilizing a combination of MR measures by adding the H-1 MRSI lateralized patients without hippocampal sensitivity of 87%, a value equal to that of FDG-PET. Figures 7 and 8 demonstrated the ability of the combined MR techniques to lateralize patients even in the absence of hippocampal atrophy. In 13 patients who underwent T2 relaxometry, lateralization was observed in 69%, as compared to 100% of these patients with FDG-PET, 77% with hippocampal volumetry, 62% with NAA/(Cr+Cho) and 69% with [NAA] shown in Table 7. 3 patients with unilateral hippocampal atrophy had abnormal T2 relaxometry. No patients with normal hippocampal volumes had abnormal T2 relaxometry.

Detection of bilateral abnormalities:
Abnormality was defined as ± 2 s.d. from the mean of controls. Of the 24 patients available for

comparison with hippocampal volumetry and H-1 MRSI, bilateral abnormalities were detected in 4 patients with HV (17%), 8 with NAA/(Cr+Cho) in 33%, and 7 with [NAA] in 29%. Of the 13 patients available to compare T2 relaxaometry, bilateral abnormalities were detected in 3 with hippocampal volumetry (23%), 6 with NAA/(Cr+Cho) in (46%), 4 with [NAA] in 31% and 1 with T2 in 8%.

Table 7 Ipsi- and contralateral NAA concentrations and NAA/(Cr+Cho) ratios (mean ± SD) in the hippocampus of NE and mTLE patients in comparison with controls (p values comparison in patients with controls).

	NAA (mM)	NAA/(Cr+Cho)
Controls (n=16)	11.6 ±1.3	0.82 ± 0.06
	NE (n=8/10)	
Ipsilateral	12.3 ± 1.9	0.79 ± 0.1
Contralateral	11.4 ± 2.7	0.78 ± 0.1
	mTLE (n=23)	
Ipsilateral	8.5 ± 1.3*	0.62 ± 0.1*
Contralateral	9.6 ± 1.3*	0.72 ± 0.1*

* indicates p value 0.001.

Metabolite imaging and correlation analysis: 24 patients had surgery. The mean follow-up was 20 months (range 15-28 months). 17 patients (71%) were seizure free (Class I); 3 had rare disability seizures (class III); and 2 had no worthwhile improvement (class IV). Lateralized hippocampal atrophy detected by hippocampal volumetry and T2 relaxometry correlated strongly ($p > 0.0001$) with seizure free outcome. FDG-PET (3 or more regions of relative hypometabolism) tended to correlate ($p > 0.07$) with good outcome (class I and II). Lateralized H-1 MRSI did not correlate with outcome.

Bilateral MR abnormalities also did not correlate with outcome. 3 patients had bilateral hippocampal artrophy. Two were seizure free and one had a class III outcome. 5 out of 7 patients with bilaterally abnormal NAA/(Cr+Cho) and 5 of 8 patients with bilaterally abnormal [NAA] were seizure free. The one patient with bilaterally abnormal T2 relaxometry was seizure free.

Table 8 NAA and NAA/(Cr+Cho) asymmetry indices (mean ± SD) of NE and mTLE patients in comparison with controls (p values compared with controls).

	Asym. NAA	Asym. NAA/(Cr+Cho)	Abs. asym. NAA	Abs. asym. NAA/(Cr+Cho)
Contr.	–0.2±4.85	0.63±6.25	3.15±5.65	4.75±3.95
NE	–4.6±7.8	–1.2±8.01	5.71±6.8	6.75±3.8
	n.s.	n.s.	n.s.	n.s.
mTLE	7.45±8.27	7.4±8.65	9.2±6.4	9.07±6.7
	p<0.001	p<0.003	p<0.001	p<0.04

Neocortical patients: Table 8 shows for NAA and NAA/(Cr+Cho) of neocortical epilepsy, mTLE and controls. In addition, [Cr} and [Cho] were calculated. The mean ipsilateral values for NAA, Cr, Cho in the neocortical patients was 12.3 ± 1.9, 9.8 ±1.2, 2.9 ± 0.7 respectively and for the mTLE patients 8.3 ± 1.3, 8.6 ± 1.6, 2.6 ± 0.4.

In contrast to mTLE, there were no significant changes in any ratio or metabolite concentrations in neocortical epilepsy compared to controls as shown in Table 8. In Figure 5, ipsilateral and contralateral values of NAA and NAA/(Cr+Cho) ratios are represented for the individual patients. In 19 out of 23 mTLE patients the ipsilateral [NAA] and NAA/(Cr+Cho) values were lower than the contralateral values. In contrast there was no uniform tendency between ipsi- and contralateral values for neocortical patients. A comparison of ipsilateral values with controls shows that for mTLE, ipsilateral [NAA] and NAA/(Cr+Cho) are significantly reduced ($p < 0.001$), whereas the mean values in neocortical epilepsy were not different from controls. Furthermore, Figures 7 and 8 showed that mTLE patients also had significantly reduced values in the contralateral hippocampus. [NAA] values and NAA/(Cr+Cho) ratios were reduced at least by ± 1.0 s.d. below the control mean in 16 patients (70% of all patients, $p > 0.0001$) and in 13 patients (57%, $p < 0.002$) respectively.

The asymmetry index (AI) was calculated to determine the degree of asymmetry between ipsi- and contralateral values of NAA and

NAA/(Cr+Cho) in neocortical epilepsy as compared to controls and mTLE shown in Table 8. In contrast to mTLE, the asymmetry of the neocortical epilepsy group did not differ significantly from controls. To detect any asymmetry independent of the location of the seizure focus, between left and right side in neocortical patients, absolute asymmetry indices were calculated. Although these asymmetry values were slightly higher in neocortical epilepsy than in controls, this difference was not significant, in contrast to the highly significant difference between mTLE and controls. Figures 6-8 represent the ipsilateral values of NAA and NAA/(Cr+Cho) for neocortical epilepsy and mTLE patients. For single patient comparison values more than ± 2 s.d. from either group (NE or mTLE) were considered to be abnormal. Ipsilateral [NAA] were reduced in 13 out of 23 mTLE patients more than ± 2 s.d. below the mean value of NE patients. On other hand, 6 out of 8 NE patients had higher [NAA] and 4 out of 10 NE patients had NAA/(Cr+Cho) values more than ± 2 s.d. above mTLE. Therefore, despite the overlap between the two groups, the metabolite values may help discriminate mTLE from NE.

Regional Variations: To observe if the location of the focus influenced the NE metabolite values, the patients were divided into 3 groups based on the relationship of their seizure focus to the hippocampus. Patients whose seizures arose from the ipsilateral frontal lobe were examined separately because of the rich, profuse ends preferred pathways between the frontal lobe and the medial temporal lobe frontal structures. All other patients were grouped together since the location of their seizure foci would be expected to have less influence on the hippocampus. No relationship between the distances of the seizure focus from the ipsilateral hippocampus (either anatomical or in terms of preferential pathways) was found for the metabolites as shown in Figure 4. Two patients without convulsions were not multiple comparisons. distinguishable from the others with respect to NAA, or NAA/(Cr+Cho) ratios.

Multislice technique: In 7 out of 9 patients (in 78%) the lateralization by MRS was concordant with EEG. NAA/(Cr+Cho) was significantly decreased in both ipsilateral and contralateral hippocampi compared to controls ($p < 0.005$). Furthermore, the asymmetry between ipsilateral and contralateral regions was highly increased ($p < 0.001$) compared to controls). Four patients (44%) had bilateral reductions in NAA/(Cr+Cho) more than ± 2 s.d. below control mean. These results confirm previous findings of reduced hippocampal NAA ipsilateral and contralateral to the seizure focus. The Figure 1 summarizes the findings of multislice study of all brain examinations. A total of 18 voxels in gray matter (9 different brain regions) were analyzed. In total, 27 ipsi-, contralateral, ipsi-control, contralateral-control examinations were tested by tail t-tests without correction for multiple comparisons. These comparisons were performed and showed in 2 voxels with tendency of reduced NAA/(Cr+Cho) on one side. However, there was no significant difference when corrected for multiple comparisons.

Discussion

A strategy of metabolite imaging and its power of prediction by using MRSI is presented. Based on MRI volume measurements were not really specific indicator of neuronal integrity. The reason is because the volume loss may reflect a variety of nonspecific mechanisms of neurodegeneration including neuronal loss, shrinkage of neuron cell bodies, or even neuronal changes such as loss of glial components. Furthermore, volume reductions may be attenuated to the extent that neurons are replaced by glia. However, the pathological neuronal loss is often accompanied by reactive gliosis.

NAA has been described as a neuronal marker because of its exclusive high concentrations in neuron cells. However, diminished NAA levels cannot be unambiguous attributed to neuronal loss. It may also reflect the dysfunction of neuronal

metabolism. Earlier reports of reversible decrease of NAA after treatment of patients with amyotrophic lateral sclerosis (ALS) or TLE are suggestive of the NAA as better indicator of neuronal loss or dysfunction than volume measurements.[20] In the case of gliosis, it reduces neuron density. It should cause further reduction of NAA levels. This presumption was in contrast to the volume measurements by MRI or metabolic rate measurements with positron emission tomography (PET) which reflect changes of both neurone and glial cells.[21] Thus, a quantitative measurement of NAA by H-1 MRSI seems to offer useful assessment of neurodegeneration.

H-1 MRSI enables the measurement of MR metabolite spectra simultaneously from multiple areas in the brain. Conventional single voxel MR spectroscopy methods are limited to a single region of interest at a time. So, H-1 MRSI is of particular importance in investigation of diffused disease such as AD showing heterogenous regional distribution of pathology. H-1 MRSI is a combination of chemical shift metabolite spectra in homogeneous magnetic field and MRI of spatial phase-encoding by stepwise increasing or decreasing magnetic field gradient pulses after slice-selection for planar MRSI.[22] After Fourier transformation of the data, each of the major peaks can then be displayed as an image, co-registered to MRI or other neuroimaging methods. H-1 MRSI technique suffers from low sensitivity and long acquisition time. These factors restrict the data sampling to a limited number of phase encoding steps. The resultant truncated sampling causes poor spatial resolution due to effect of "voxel bleeding"[23] as a result of contamination of brain metabolite MR spectra with intense lipid resonances originated from outside the brain i.e. skull.

The primary limitation of volume preselection using PRESS is that outer cortex of the brain is difficult to sample and only one slice is studied at a time. Multislice MRSI extends coverage to regions of the outer cortex, using spatially localized saturation pulses to suppress the resonances from skull lipids. However, a problem of these saturation pulses is that they may also affect metabolite resonances in the outer cortex, complicating the quantitation of metabolite concentration in this region. However, data processing method was reported accomplished by extrapolating the measured spatial frequency distribution selectively from the skull lipids to a wider range. It resulted with less "voxel bleeding" for these lipid resonances and less contamination to generate better brain metabolite images.[24]

Alzheimer's disease: Noninvasive diagnosis of AD has been a partial success story by using H-1 MRSI demonstrating global cerebral atrophy and reduced hippocampus valumes. However, there is reported overlap between AD patients and nondemented elderly subjects.[25]

In present paper, H-1 MRSI study of supraventricular regions in the fronto-parietal brain in AD showed reduced NAA levels when compared with controls. NAA reduced levels remain independent of unpredictable tissue composition measured by MRI, which also corroborates with earlier reports.

Data correction for tissue atrophy and for variations of tissue composition provides the opportunity that NAA reductions in AD occur independently from structural variations as measured by MRI. In both right and left hippocampus regions in AD, atrophy corrected NAA levels were reduced when compared with age-matched controls. Earlier, such reduced NAA levels and hippocampal volumes were suggestive of hippocampal lateralization as good noninvasive tool.[25]

So, hippocampal NAA measured by H-1 MRSI combined with measurements of hippocampal volume by MRI may improve diagnosis.[24,25] Similarly, outer cortex regions in AD were analyzed for reduced NAA levels in GM of parietal and frontal cortex by regression method using extrapolation when compared with controls shown in Figure 8. These findings were further confirmed by histogram distribution of the NAA levels in parietal cortex.

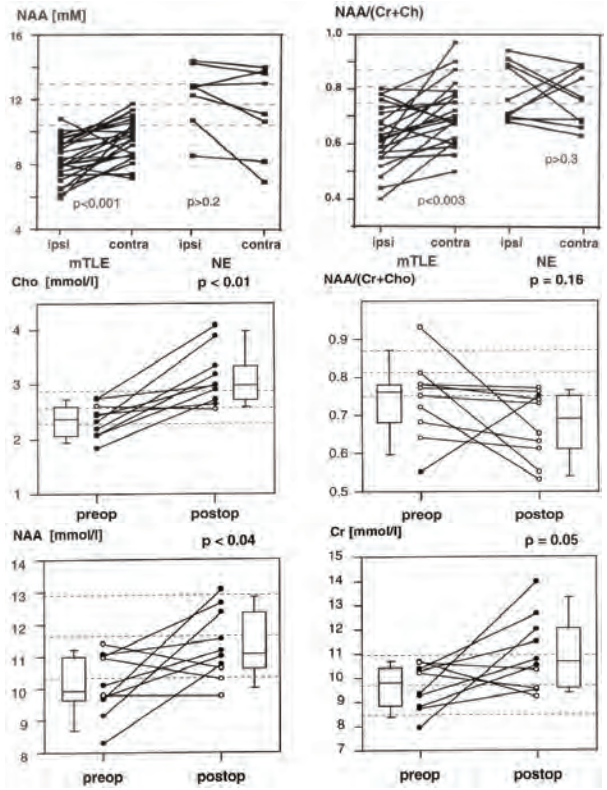

Figure 8 Metabolite status of NAA and NAA/(Cr+Cho) in mTLE and neocortical epilepsy is shown in ipsi- and contralateral sides of brain.

Epilepsy: In TLE, the seizure focus was localized in hippocampus.[26] For surgical treatment of TLE, the determination of location and size of the focus is important for knowing the extent of affected other brain regions.[27] MRI, PET and H-1 MRS are methods of choice to evaluate TLE.[28] H-1 MRSI using PRESS was commonly used to measure metabolite changes in regions of the mesial temporal lobe, including hippocampus.[29-31] Present paper highlights the importance of lateralization of hippocampus (affected by seizure) using spectra from left and right hippocampi with depleted NAA intensity. These NAA levels were depleted in ipsilateral hippocampus and temporal lobe of TLE patients. However, TLE patients had reduced NAA levels in the hippocampus contralateral to the seizure focus, when compared with controls. It can be attributed due to bilateral mesial temporal sclerosis or due to repeated seizure activity.[32] If reduced seizure activity is responsible for reduced NAA levels at the contralateral side, the NAA might also be reduced in other regions of hippocampus.[33] It suggests metabolite change or neuronal damage. Multislice H-1 MRSI predicted well the regional differences of NAA/(Cho+Cr) ratio of the hippocampus i.e. lower ratio on the ipsilateral side of the seizure focus than the contralateral side in the present study. Moreover, many ipsilateral brain regions of TLE patients showed lower values of NAA/(Cho+Cr) and averaged NAA/(Cho+Cr) than in the corresponding brain regions of control subjects. This may be attributed that repeated seizures originating from the hippocampus may eventually lead to impairmrnt of other brain regions.[34] This information from multislice H-1 MRSI might help the lateralization of the seizure focus.

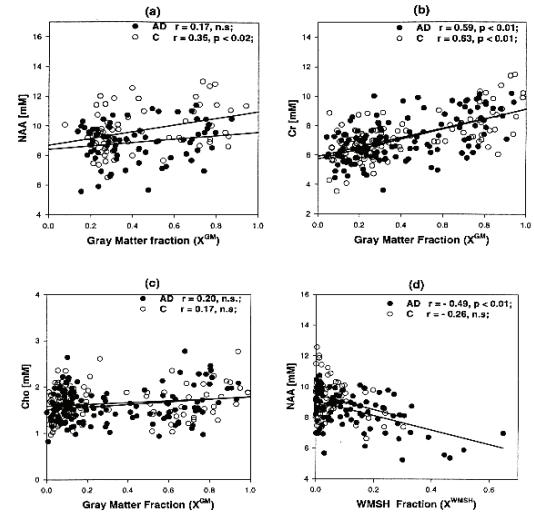

Figure 9 Regression analysis of metabolites and tissue fraction analysis for NAA and Cr, cho and white and gray matter in AD.

MRSI data analysis by "voxel selection" uses anatomical landmarks obtained from MRI. Due to operator bias and reading variability, voxel selection becomes complicated especially in diffused diseases like Alzheimer's disease. Multislice H-1 MRSI with completely automated spectral fitting and co-registered MRI segmentation appears free from operator-dependent variability. The method has power of tissue volume correction and quantitation of

metabolites and tissue composition. Despite it, the method suffers from a number of limitations. First, H-1 MRSI slices are not contiguous and method uses long echo times more than 130 msec. However, shorter echo time is associated with increased lipid and water contamination. In order to suppress lipids and water contamination, very uniform magnetic field homogeneity across the brain is needed. In brain lower-anterior regions of the brain shimming is a problem. However, H-1 MRSI is practical, feasible and provides metabolic and anatomical information from MRI useful in clinical decision-making.

Acknowledgements

Author acknowledges the facility and visiting faculty fellowship provided by Professor Michael W. Weiner at DVA Medical Center, San Francisco, Magnetic Resonance Spectroscopy Center, University of California, San Francisco CA.

Literature

1. Tanabe JL, Amend D, Schuff N et al. Tissue segmentation of the brain in Alzheimer disease Am.J.Neurol.Res. 1997; 18;115-123.
2. Kesslak JP, Nalcioglu O, Cotman CW Quantification of magnetic resonance scans for hippocampal and parahippocampal atrophy in Alzheimer's disease. Neurology 1991; 41;51-54.
3. Jack CR,Peterson CR, O'Brien PC et al. Rates of hippocampal atrophy correlate with change in clinical status in aging and AD Neurology 1992;42; 183-188.
4. Knowlton RC, Laxer KD, Ende G et al. Presurgical multimodality neuroimaging in electroencephalographic lateralized temporal lobe epilepsy Ann Neurol. 1997; 42(4):829-837.
5. Urenjak J, Williams SR, Gadian DG, et al. Proton nuclear magnetic resonance spectroscopy unambiguously identifies different neural cell types *J.Neurochem.* 1992;59;55-61.
6. Kalra S, Cashman NR, Genge A, Arnold DL Recovery of N-acetylaspartate in corticomotor neurons of patients with ALS after riluzole therapy *Neuroreport* 1998;9,1757-1761.
7. Hugg JW,Kuziecky RI, Gilliam FG,Morawetz RB et al. Normalization of contralateral metabolic function following temporal lobectomy demonstrated by 1H magnetic resonance spectroscopic imaging *Ann Neurol*.1996;40,236-239.
8. Cendes F,Andermann F, Dubeau F,Matthews PM,Arnold DL Normalization of neuronal metabolic dysfunction after surgery for temporal lobe epilepsy. Evidence from proton MR spectroscopic imaging. *Neurology*. 1997;49(6):1525-33.
9. Chang L,Ernst T, Relationships among brain metabolites, cognitive function, and viral loads in antiretroviral-naive HIV patients *Neuroimage*. 2002 Nov;17(3):1638-48.
10. Bottomley PA, Selective volume method for performing localized NMR spectroscopy US patent 4 1995; 480 228.
11. Young K, Govindraju V, Soher BJ, Maudsley AA. Automated spectral analysis III: application to in vivo proton MR spectroscopy and spectroscopic imaging. *Magn Reson Med* 1998; 40,812-815.
12. Soher BJ, Vermathen P, Schuff N, et al. Short TE in vivo (1)H MR spectroscopic imaging at 1.5 T: acquisition and automated spectral analysis. *Magn Reson Imaging*. 2000;18(9):1159-65.
13. Soher BJ, Young K, Govindraju V, Maudsley AA Representation of strong baseline contributions in 1H MR spectra *Magn Reson Med*. 2001;45(6):966-72.
14. MacKay S, Ezekiel F, Di Sclafani V, Meyerhoff DJ et al. Alzheimer disease and subcortical ischemic vascular dementia: evaluation by combining MR imaging segmentation and H-1 MR spectroscopic imaging. *Radiology*. 1996;198(2):537-45.
15. MacKay S,Meyerhoff DJ,Constans JM et al. Regional gray and white matter metabolite differences in subjects with AD, withsubcortical ischemic vascular dementia, and elderly controls with 1H magnetic resonance spectroscopic imaging *Arch Neurol* 1996;53;167-174.
16. Schuff N, Amend D,Ezekiel, Steinman SK,Tanabe J et al. Changes of hippocampal N-acetyl aspartate and volume in Alzheimer's disease. A proton MR spectroscopic imaging and MRI study *Neurology* 1997; 49(6);1513-1521.
17. Schuff N, Amend D,Meyerhoff DJ et al. Alzheimer disease: quantitative H-1 MR spectroscopic imaging of frontoparietal brain.*Radiology*. 1998;207(1):91-102.

18. Ende GR, Laxer KD, Knowlton RC, Matson GB,et al Temporal lobe epilepsy: bilateral hippocampal metabolite changes revealed at proton MR spectroscopic imaging. *Radiology*. 1997;202(3):809-17.
19. Vermathen P, Ende G, Laxer KD, et al. Temporal lobectomy for epilepsy: recovery of the contralateral hippocampus measured by (1)H MRS *Neurology*. 2002 Aug 27;59(4):633-6.
20. Mielke R, Schopphoff HH, Kugel H, Pietrzyk U, et al. Relation between 1H MR spectroscopic imaging and regional cerebral glucose metabolism in Alzheimer's disease. *Int J Neurosci.* 2001;107(3-4):233-45.
21. Constans JM, Meyerhoff DJ, Gerson J, et al. H-1 MR spectroscopic imaging of white matter signal hyperintensities: Alzheimer disease and ischemic vascular dementia.*Radiology*. 1995;197(2):517-23.
22. Block W, Traber F, Kuhl CK, Fric M, Keller E, et al. 1H-MR spectroscopic imaging in patients with clinically diagnosed Alzheimer's disease] *Rofo Fortschr Geb Rontgenstr Neuen Bildgeb Verfahr*. 1995;163(3):230-7.
23. Kuzniecky R, Palmer C, Hugg J, Martin R,et al. Magnetic resonance spectroscopic imaging in temporal lobe epilepsy: neuronal dysfunction or cell loss? *Arch Neurol*. 2001;58(12):2048-53.
24. Serles W, Li LM, Antel SB, Cendes F,et al. Time course of postoperative recovery of N-acetyl-aspartate in temporal lobe epilepsy.*Epilepsia*. 2001;42(2):190-7.
25. Capizzano AA, Vermathen P, Laxer KD,et al. Temporal lobe epilepsy: qualitative reading of 1H MR spectroscopic images for presurgical evaluation.*Radiology*. 2001;218(1):144-51.
26. Li LM, Cendes F, Andermann F, Dubeau F, Arnold DL. Spatial extent of neuronal metabolic dysfunction measured by proton MR spectroscopic imaging in patients with localization-related epilepsy. *Epilepsia*. 2000;41(6):666-74.
27. Vermathen P, Laxer KD, Matson GB, Weiner MW. Hippocampal structures: anteroposterior N-acetylaspartate differences in patients with epilepsy and control subjects as shown with proton MR spectroscopic imaging.*Radiology*. 2000;214(2):403-10.
28. Serles W, Li LM, Caramanos Z, Arnold DL, Gotman J. Relation of interictal spike frequency to 1H-MRSI-measured NAA/Cr. *Epilepsia*. 1999 ;40(12):1821-7.
29. Hsu YY, Chang C, Chang CN et alProton MR spectroscopy in patients with complex partial seizures: single-voxel spectroscopy versus chemical-shift imaging. *AJNR Am J Neuroradiol*. 1999;20(4):643-51.
30. Kuzniecky R, Hugg JW, Hetherington H et al. Relative utility of 1H spectroscopic imaging and hippocampal volumetry in the lateralization of mesial temporal lobe epilepsy. *Neurology*. 1998 Jul;51(1):66-71.
31. Stanley JA, Cendes F, Dubeau F, Andermann F, Arnold DL. Proton magnetic resonance spectroscopic imaging in patients with extratemporal epilepsy. *Epilepsia*. 1998;39(3):267-73.
32. Li LM, Cendes F, Bastos AC, Andermann F et al. Neuronal metabolic dysfunction in patients with cortical developmental malformations: a proton magnetic resonance spectroscopic imaging study.*Neurology*. 1998;50(3):755-9.
33. Cendes F, Caramanos Z, Andermann F, et al. Proton magnetic resonance spectroscopic imaging and magnetic resonance imaging volumetry in the lateralization of temporal lobe epilepsy: a series of 100 patients. *Ann Neurol*. 1997;42(5):737-46.
34. Achten E, Boon P, Van De Kerckhove T et al. Value of single-voxel proton MR spectroscopy in temporal lobe epilepsy.*AJNR Am J Neuroradiol*. 1997;18(6):1131-9.